ORIGINAL ARTICLE

Patellar calcar: morphometric analysis by knee magnetic resonance imaging and three-dimensional reconstruction software-assisted

Sergio Benavente[1] · Joaquín Villagra[1]

Abstract

Purpose Patellar calcar corresponds to a greater trabecular bone density area in the patella lateral facet, whose morphometry is uncertain. This study aimed to describe patellar calcar morphometry by knee MRI and develop a 3D reconstruction software-assisted.

Materials and methods Consecutive adult patients, submitted to knee MRI, between 2014 and 2017, were entered in IMPAX software. Exclusion criteria are history of patellar surgical intervention, trauma, chondromalacia, bone edema or bipartite patella. All MRI images were retrospectively reviewed by three readers. MRI patellar calcar measurements are height, width, thickness and posterior distance. 3D model protocol reconstruction: 3D Slicer software was used to design a preliminary model for each patient, and then all were automatically merged into one, which was finalized using the software segmentation tools. For 3D patellar calcar location, the transpolar axis was designed.

Results 250 MRI were analyzed, patellar calcar was present in 208 (83.2%); 101 men and 107 women. Mean age was 44.3 ± 15.6 years. Measurements: height 13.84 ± 2.42 mm (male: 14.50 ± 2.42; female: 13.21 ± 2.26) ($p < 0.0001$), width 12.21 ± 2.26 mm (male 13.14 ± 2.22; female 11.33 ± 1.93) ($p < 0.0001$). No statistically significant difference of thickness 0.56 ± 0.22 mm (male: 0.56 ± 0.25; female: 0.56 ± 0.20) and posterior distance 2.37 ± 0.80 mm (male: 2.46 ± 0.89; female: 2.29 ± 0.69) between genders was found. 3D model results: transpolar axis went through the patellar calcar in all the cases.

Conclusions This study shows in a 3D model reconstruction, what was previously described in the literature, determining for the first time the patellar calcar morphometry in the knee MRI and identifying it as a regular finding in this imaging test.

Keywords Patella · Calcar · Patellar calcar · Knee · Magnetic resonance imaging · MRI

Introduction

The mechanical stimuli in the bone, that are received over a long period of time, adapt and remodel the bone tissue for optimal forces' distribution, process known as Wolff's law [23, 28]. To comprehend the changes within the bony structures, one has to understand the normal biomechanics of the knee joint. Due to the external rotation of the tibial tuberosity in maximal extension of the knee, the Q-angle is maximized and the lateral facet has the most contact area with the femur condyle [2, 9, 13]. The medial facet comes into contact from 20° flexion and toward the 90° flexion the contact area is like a narrow band. Flexion toward 135°

shows a change in contact pressure, the medial facet lies free and only the proximal part of the lateral facet and the odd facet engages the femur [1, 10, 11, 24, 25]. In consequence, the lateral facet contact area is about 60% greater than the medial, hence, suggesting a higher load-bearing capacity for the lateral surface and for a long period of time [3, 8, 14–16].

The differences in the density distribution throughout the patella joint surface has been described, which also follows a regular distribution pattern [6, 7, 17, 18, 20], having its maximum thickness on the lateral facet, and even a specific trabeculae architecture [26, 27].

Recently, this greater area of trabecular bone density has been described in knee magnetic resonance (MRI) as a dark signaling with a curvilinear structure with anterior convexity located in the lateral facet of the patella [5], and named patellar calcar (PC) after the femoral calcar which is a constant anatomical structure representing a condensation of bone trabeculae [12, 19]. It has a prevalence of 81%

✉ Joaquín Villagra
jorivillaj@gmail.com

1 Universidad Católica de la Santísima Concepción, Concepción, Chile

and is a non-pathological entity, but whose morphometry is uncertain.

Objective

The aim of this study is to describe PC morphometry by MRI and develop a three-dimensional (3D) reconstruction software-assisted.

Methods

After institutional review board approval, a cross-sectional study was carried out including consecutive adult patients, submitted to knee MRI, at the same center, between 2014 and 2017, entered in IMPAX software, version 6.3.1.8000 of the AFGA Healthcare provider. Exclusion criteria are history of fracture or patellar trauma, patellar surgical intervention, chondromalacia patellae, bipartite patella or patellar bone edema.

PC was previously defined as "curvilinear structure with anterior convexity that gives a hypointense signal and is best observed in proton density weighted and without fat suppression, which is located in the lateral facet of the patella" [5] (Fig. 1).

MRI protocol

All MRI were performed by Philips Ingenia model 1.5 Tesla with acquisition of images of 3 mm every 3 mm. MRI protocol: Patient in supine position, entering the feet first, with a knee flexion of 15°, immobilized with cushions, using a knee quadrature coil, locating the lower edge of the patella to the coil center. This protocol includes the following planes and sequences: in sagittal, axial and coronal images in proton density-weighted (PDW) and T1-weighted (T1), both in Turbo Spin Echo (TSE) and Spectral Attenuated Inversion Recovery (SPAIR). The complete proton density-weighted MRI sequences' description is detailed in Table 1.

MRI analysis

For the purposes of this study and for standardization, the PC was defined just as Collin et al. [5] did, as the presence of a dark signaling, linear or curvilinear structure subjacent to the patellar articular surface and is best observed in PDW without fat suppression. All the measures were performed in that sequence. All MRI images were reviewed in consensus in three different occasions by a board conformed by a senior musculoskeletal radiologist, an orthopedic surgeon with experience in knee MRI and an assistant researcher after training. The images were reviewed initially to determine if a calcar was or was not present. With IMPAX program tools, the level of

Fig. 1 A 19-year-old woman knee MRI in PDW sequence without fat suppression, axial plane (left) and sagittal (right). Arrows indicating PC: curvilinear structure with anterior convexity of hypointense signal in the lateral facet of the patella
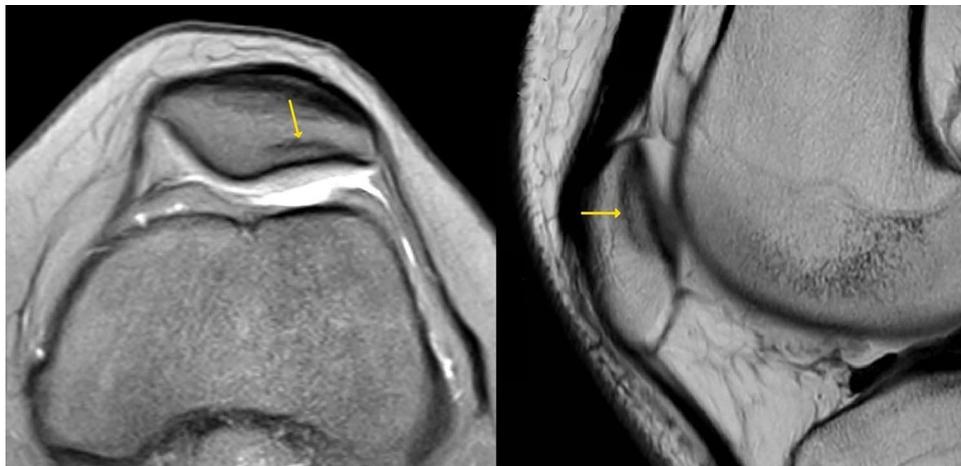
Table 1 MRI sequences description

Sequence	Slices	Repetition time (TR) (ms)	Echo time (TE) (ms)	Flip angle	Echo spacing (ms)	Refocusing control	Fat suppression
PDW_TSE	22	2000	30	90°	8	Constant in 120°	No
PDW_SPAIR	22	3205	30	90°	8	No	SPAIR

contrast was increased, the image was enlarged, and the screen was divided to analyze the same anatomical point simultaneously in the axial, sagittal and coronal projections. Location of the calcar within the patella, orientation relative to the posterior cortical surface of the body of the patella, general configuration and the following measurements were recorded.

Measurements

PC thickness (A)

A is measured at the midpoint of the PC in the sagittal plane, from the anterior edge to the posterior edge of the hypointense signal (Fig. 2).

PC height (B)

B is measured in the longest cut of the PC in the sagittal plane, from the upper pole to the lower pole of the hypointense signal (Fig. 2).

PC width (C)

C is measured in the longest cut of the PC in the axial plane, from the external pole to the internal pole of the hypointense signal (Fig. 3).
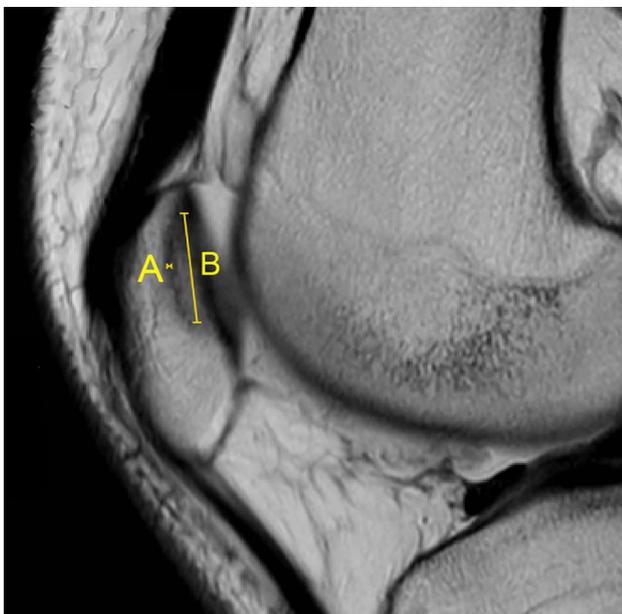

Fig. 3 A 19-year-old woman knee MRI in PDW sequence without fat suppression, axial plane. C: PC width. D PC posterior distance

PC posterior distance (D)

D is measured at the midpoint of the PC in the axial plane, from the subchondral bone of the lateral facet of the patella to the posterior edge of the hypointense signal (Fig. 3).

Statistical analysis

The *t* student statistical test (SPSS software) was used to compare the PC morphometry in male and female gender, with a 95% of confidence interval.

Reconstruction protocol to 3D model

All the MRI images obtained from the IMPAX program were downloaded in DICOM format and loaded in the 3D Slicer software version 4.8.1 for Windows 10 without losing resolution. A preliminary model of each patient was made. PC is best observed in the sagittal axis [5]. A four-up divided screen tool was used to see the same marked point in the sagittal plane, simultaneously in the axial and coronal axis, and visualize it in the 3D model reconstruction. The complete PC contour was marked on the sagittal axis, and the marks were rendered in the other planes, and the 3D model was generated automatically. The length and width were marked following the shape of the PC, at the same time a central point was defined as the intersection between the length and width marks. All preliminary models were imported to a master volume of a DICOM format MRI with a field of view of 140 mm high × 140 mm

Fig. 2 A 19-year-old woman knee MRI in PDW sequence without fat suppression, sagittal plane. A: PC thickness. B: PC height

long × 155 mm wide, a voxel of $0.68 \times 0.68 \times 0.68$ mm, 208 cuts in axial, 206 cuts in coronal and 228 cuts in sagittal, without empty spaces between each cut. All the preliminary models of left knees were flipped horizontally to obtain only right knee models, and then the central point of PC was used to match all the models and get a single reconstruction model. At this point, the less dense area of the grouped patella was trimmed with the scissors tool; thereupon merged leaving a single model. As well, the PC was finalized with the tool of filling between cuts, and then the model was smoothed closing holes and eliminating extrusions with the smoothing tool, creating a single PC. The merged patella was smoothed a last time to get rid of extrusions and holes with the smoothing tool, creating a final reconstruction model.

Measurements in the 3D model for PC localization

After obtaining the preliminary 3D reconstruction models of each patient, the following measurement was designed for PC localization.

Transpolar axis

It is defined as a transverse axis from the superolateral patellar pole to the superomedial patellar pole (Fig. 4).
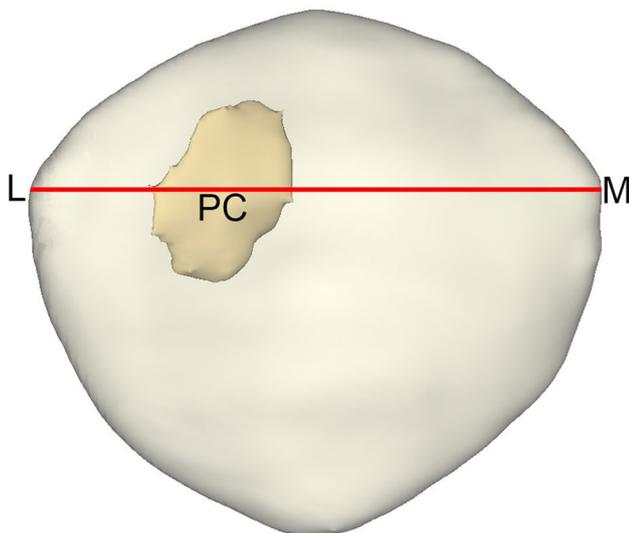

Fig. 4 Three-dimensional reconstruction frontal view of the PC in the patella. *PC* Patellar calcar. L: superolateral patellar pole. M: superomedial patellar pole. LM: transpolar axis

Results

Characteristics of the patients

A total of 250 MRIs were analyzed; of these, PC was present in 208 patients (83.2%). The clinical characteristics of the patients are shown in Table 2. The mean age was 44.3 ± 15.6 years. 101 patients (48.6%) were male and 107 patients (51.4%) were female. For the laterality, 125 (60.1%) were right and 83 (39.9%) were left.

MRI

The PC was located on the lateral facet subjacent to the articular surface in all cases; it is located in a superior and medially position, not in the center of the facet. In the sagittal plane, it is observed as a curvilinear structure (Fig. 1), whereas in the axial plane, it has a more linear conformation (Fig. 1). It is observed only in the axial and sagittal planes; in the coronal plane, it is not possible to see due to its orientation and thickness.

Measurements

The morphometric PC results according to MRI are detailed in Table 3. The average height of the PC was 13.84 ± 2.42 mm and the mean width was 12.21 ± 2.26 mm. Therefore, the PC is taller than wide. There was a significant statistically difference in height ($p < 0.0001$) and width ($p < 0.0001$) according to gender, being higher in men than in women.

The average thickness of the PC was 0.56 ± 0.22 mm and the mean posterior distance 2.37 ± 0.80 mm. For both measures, there was no statistically significant difference between genders.

3D model

A 3D model was developed and shown in Figs. 4 and 5. In this reconstruction model, the PC and its relation with the patella are clearly observed. PC has a more prominent curvature in the sagittal axis, as it can be seen in both lateral and superior views; in the first one, the PC is seen as a curved

Table 2 Sample description

	Total ($n = 208$)	Male ($n = 101$)	Female ($n = 107$)
Mean age[a]	44.3 ± 15.6	42.1 ± 17.2	46.3 ± 13.8
Right patella	125	64	61
Left patella	83	37	46

[a]Age in years ± standard deviation

Table 3 Patellar calcar morphometry

Measurements[a]	Total (n = 208)	Male (n = 101)	Female (n = 107)	p value[b]
Thickness (A)	0.56 ± 0.22	0.56 ± 0.25	0.56 ± 0.20	0.9
Height (B)	13.84 ± 2.42	14.50 ± 2.42	13.21 ± 2.26	< 0.0001
Width (C)	12.21 ± 2.26	13.14 ± 2.22	11.33 ± 1.93	< 0.0001
PC posterior distance (D)	2.37 ± 0.80	2.46 ± 0.89	2.29 ± 0.69	0.1

[a]Measures in mm ± standard deviation

[b]95% interval of confidence
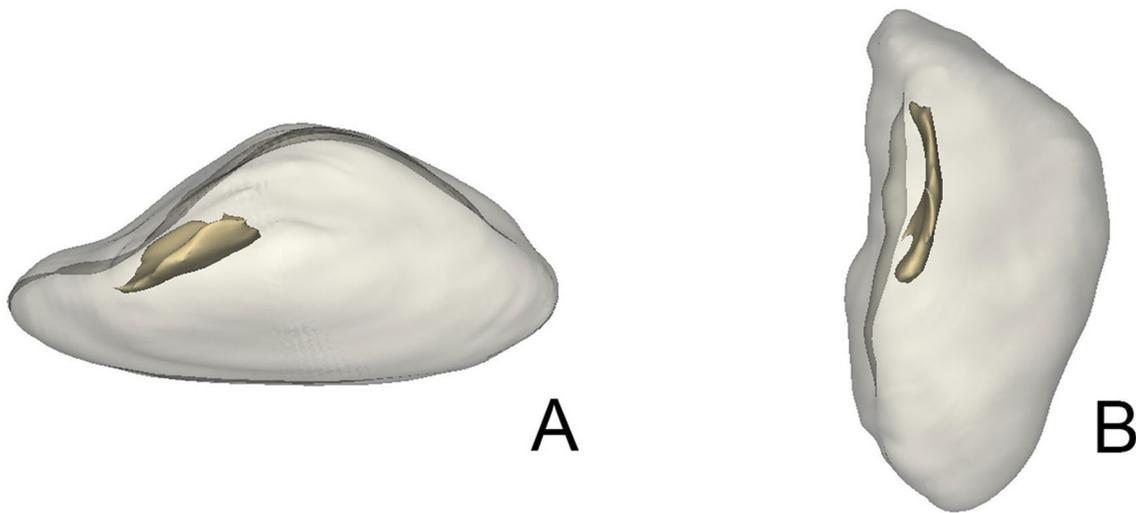
Fig. 5 Three-dimensional PC reconstruction using 3D Slicer software. Upper view of PC in the patella (**a**); lateral view of PC in the patella (**b**)

line, whereas in the last one, both the superior and lower PC poles can be observed. Overall, it has a similar shape to the lateral facet, with an anterior convexity and irregular edges. For PC location, the transpolar axis went through the PC in all the cases (Fig. 4).

Discussion

According to Wolff [28], bone is a tissue capable of adapting its structural condition depending on the biomechanical requests to which it is exposed [4, 21, 22]. The patellofemoral biomechanics determines that the contact area and distribution of loads in the lateral facet of the patella are consistently greater than the medial [3, 8, 14–16]. Eckstein et al. [7] reported through computed tomography analysis, a heterogeneous distribution of the subchondral bone density of the patella, with a high-density concentric pattern in the upper area of lateral facet. Toumi et al. [27] studied patellar trabecular architecture through histological sections, finding an increase in the number and thickness of the trabeculae in the lateral facet respect to medial. Hoechel et al. [17], using computerized microtomography, described an increase in bone density in the lateral facet, reporting an isotropic

constellation in this area. By the other hand, Collins et al. [5], analyzed for the first time the PC by MRI, defining it as a "hypointense signal of curvilinear shape with anterior convexity, which is better observed in weighted of proton density and without fat suppression, in the lateral facet of the patella", present in 81% of his series, similar to our results (83.2%).

The 3D morphometry of PC has not been previously described (Figs. 4, 5). It is a structure of irregular edges, located in the medial, superior and posterior region of the lateral facet, at a mean distance of 2.37 ± 0.80 mm from the subchondral bone (D). Its distribution presents a posterior concavity that follows the shape of the facet (Fig. 5). It has a thickness of 0.56 ± 0.22 mm (A), height 13.84 ± 2.42 mm (B) and width 12.21 ± 2.26 mm (C) (Table 3, showing a statistically significant difference in PC height ($p < 0.0001$) and width ($p < 0.0001$) according to gender, being higher in men than in women. On the other hand, PC presents similar values of thickness and posterior distance between genders (Table 3).

For its location, the transpolar axis has been defined as a transverse axis from the superolateral patellar pole to the superomedial patellar pole, which went through the PC in all the cases (Fig. 4).

This study shows in a 3D model, what was previously described in the literature [5, 7, 17, 27], determining for the first time the PC morphometry in the knee MRI and identifying it as a regular finding in this imaging test.

Author contribution Protocol/project development: SB, JV. Data collection and management: SB, JV. Data analysis: SB, JV. Manuscript writing/editing: SB, JV.

Compliance with ethical standards

Conflict of interest The authors declare that they have no conflicts of interest.

References

1. Ahmed A, Burke D (1983) In-vitro of measurement of static pressure distribution in synovial joints—part I: tibial surface of the knee. J Biomech Eng 105(3):216. https://doi.org/10.1115/1.3138409

2. Amis A, Senavongse W, Bull A (2006) Patellofemoral kinematics during knee flexion–extension: an in vitro study. J Orthop Res 24(12):2201–2211. https://doi.org/10.1002/jor.20268

3. Borotikar B, Sheehan F (2013) In vivo patellofemoral contact mechanics during active extension using a novel dynamic MRI-based methodology. Osteoarthr Cartil 21(12):1886–1894. https://doi.org/10.1016/j.joca.2013.08.023

4. Burr D, Martin R, Schaffler M, Radin E (1985) Bone remodeling in response to in vivo fatigue microdamage. J Biomech 18(3):189–200. https://doi.org/10.1016/0021-9290(85)90204-0

5. Collins M, Tiegs-Heiden C, Stuart M (2013) Patellar calcar: MRI appearance of a previously undescribed anatomical entity. Skelet Radiol 43(2):219–225. https://doi.org/10.1007/s00256-013-1776-3

6. Eckstein F, Milz S, Anetzberger H, Putz R (1998) Thickness of the subchondral mineralised tissue zone (SMZ) in normal male and female and pathological human patellae. J Anat 192(1):81–90. https://doi.org/10.1046/j.1469-7580.1998.19210081.x

7. Eckstein F, Müller-Gerbl M, Putz R (1992) Distribution of subchondral bone density and cartilage thickness in the human patella. J Anat 180(Pt 3):425–433

8. Fitzpatrick C, Baldwin M, Ali A, Laz P, Rullkoetter P (2010) Comparison of patellar bone strain in the natural and implanted knee during simulated deep flexion. J Orthop Res 29(2):232–239. https://doi.org/10.1002/jor.21211

9. Fox A, Wanivenhaus F, Rodeo S (2012) The basic science of the patella: structure, composition, and function. J Knee Surg 25(02):127–142. https://doi.org/10.1055/s-0032-1313741

10. Fulkerson JP, Hungerford DS (1990) Disorders of the Patellofemoral Joint, 2nd edn. Williams & Wilkins, Baltimore

11. Grelsamer R, Klein J (1998) The biomechanics of the patellofemoral joint. J Orthop Sports Phys Ther 28(5):286–298. https://doi.org/10.2519/jospt.1998.28.5.286

12. Griffin J (1982) The calcar femorale redefined. Clin Orthop Relat Res 164:211–214. https://doi.org/10.1097/00003086-198204000-00036

13. Heegaard J, Leyvraz P, Curnier A, Rakotomanana L, Huiskes R (1995) The biomechanics of the human patella during passive knee flexion. J Biomech 28(11):1265–1279. https://doi.org/10.1016/0021-9290(95)00059-q

14. Hefzy M, Yang H (1993) A three-dimensional anatomical model of the human patello-femoral joint, for the determination of patello-femoral motions and contact characteristics. J Biomed Eng 15(4):289–302. https://doi.org/10.1016/0141-5425(93)90005-j

15. Hefzy M, Jackson W, Saddemi S, Hsieh Y (1992) Effects of tibial rotations on patellar tracking and patello-femoral contact areas. J Biomed Eng 14(4):329–343. https://doi.org/10.1016/0141-5425(92)90008-9

16. Hehne H (1990) Biomechanics of the patellofemoral joint and its clinical relevance. Clin Orthop Relat Res. https://doi.org/10.1097/00003086-199009000-00011

17. Hoechel S, Schulz G, Müller-Gerbl M (2015) Insight into the 3D-trabecular architecture of the human patella. Ann Anat 200:98–104. https://doi.org/10.1016/j.aanat.2015.02.007

18. Hoechel S, Wirz D, Müller-Gerbl M (2012) Density and strength distribution in the human subchondral bone plate of the patella. Int Orthop 36(9):1827–1834. https://doi.org/10.1007/s00264-012-1545-2

19. Le Corroller T, Dediu M, Pauly V, Pirro N, Chabrand P, Champsaur P (2011) The femoral calcar: a computed tomography anatomical study. Clin Anat 24(7):886–892. https://doi.org/10.1002/ca.21177

20. Milz S, Eckstein F, Putz R (1995) The thickness of the subchondral plate and its correlation with the thickness of the uncalcified articular cartilage in the human patella. Anat Embryol. https://doi.org/10.1007/bf00240376

21. Müller-Gerbl M, Putz R, Hodapp N, Schulte E, Wimmer B (1989) Computed tomography-osteoabsorptiometry for assessing the density distribution of subchondral bone as a measure of long-term mechanical adaptation in individual joints. Skeletal Radiol 18(7):507–512. https://doi.org/10.1007/bf00351749

22. Müller-Gerbl M, Putz R, Hodapp N, Schulte E, Wimmer B (1990) Demonstration of subchondral density pattern using CT-osteoabsorptiometry (CT-OAM) for the assessment of individual joint stress in live patients. Z Orthop Unf 128(02):128–133. https://doi.org/10.1055/s-2008-1039487

23. Pauwels F (1965) Gesammelte Abhandlungen zur funktionellen Anatomie des Bewegungsapparates. Springer, Berlin

24. Salsich GB, Ward SR, Terk MR, Powers CM (2003) In vivo assessment of patellofemoral joint contact area in individuals who are pain free. Clin Orthop Relat Res. https://doi.org/10.1097/01.blo.0000093024.56370.79

25. Seisler A, Sheehan F (2007) Normative three-dimensional patellofemoral and tibiofemoral kinematics: a dynamic, in vivo study. IEEE Trans Biomed Eng 54(7):1333–1341. https://doi.org/10.1109/tbme.2007.890735

26. Toumi H, Higashiyama I, Suzuki D, Kumai T, Bydder G, McGonagle D et al (2006) Regional variations in human patellar trabecular architecture and the structure of the proximal patellar tendon enthesis. J Anat 208(1):47–57. https://doi.org/10.1111/j.1469-7580.2006.00501.x

27. Toumi H, Larguech G, Filaire E, Pinti A, Lespessailles E (2012) Regional variations in human patellar trabecular architecture and the structure of the quadriceps enthesis: a cadaveric study. J Anat 220(6):632–637. https://doi.org/10.1111/j.1469-7580.2012.01500.x

28. Wolff J (1892) Das Gesetz der transformation der Knochen. Hirschwald, Berlin